DIGITAL MAGNETIC IMAGING OF STEEL CORD CONVEYOR BELTS

MJ Alport, JF Basson and T Padayachee

1. INTRODUCTION

Steelcord-reinforced conveyor belting is widely used for the transportation of various products (e.g. coal and ash in power stations) particularly for long overland conveyors. The ability to perform continuous non-destructive condition monitoring of these belts would be beneficial to improve the reliability and availability of these belt transport systems.

Although X-ray technology has been successfully employed for the online imaging of cord and splice defects in steel cord-reinforced belting [1], both the high cost of such systems combined with safety issues due to the radiation hazard, discourages their use for permanent installations. Thus, X-ray systems are predominantly used for surveying belts, typically every 6 months. Clearly, in this survey mode, corrective action cannot be implemented for events that occur on a timescale shorter than 6 months. Another alternative technique [2] that was developed some time ago measures the magnetic fringing fields that occur above breaks in previously magnetised cords. Initial implementations of this technology relied on a relatively few sensors and because these sensors were mostly coils, their output was proportional to the rate of change of the magnetic field. This signal, typically viewed on a chart recorder, was often difficult to interpret.

In March 2006, Advanced Imaging Technologies (AIT) began the development of a new second generation magnetic technology [3], called MYRIAD™. This technology uses an array of magnetic field (B-field) sensors that measures the local value of the magnetic field directly, and can give a high resolution image of belt damages and splices.

1.1 PREVIOUS WORK

In the 1970's, Dr. Alex Harrison (Australian CSIRO) developed CBM, for Conveyor Belt Monitoring, which used a U-shaped yoke placed across the moving belt and excited at between 50 Hz and 50 kHz. The strength of the signal detected by a receiving coil was dependent on the permeability of the region in front of the pole faces, including the belt cords.

EyeQ has been developed by Fenner Vulcanisers International, United Kingdom uses 4 sensors mounted transversally across the belt.

The QTI Group (Canada) developed CAT (Belt Cable Anomaly Tomography) which uses 4 scanner heads, which are placed across the belt and generate opposing oscillating magnetic fields in two longitudinally spaced coils. Hall effect sensors, placed at a spacing of 1 cm across the belt, generate an image of the steel cord carcass. If there is any anomaly that affects the difference in permeability of one coil with respect to the other (for example, by a cord break), then the sensors generate a signal.

More recently, Rescan Pty Ltd, an Australian company, uses a set of two 'conditioning transducers' (permanent magnets) and one 'sense transducer' (series wound coils). Any breaks or corrosion produce small magnetic fields that induce voltages within the sense transducer.

The current magnetic imaging technology differs from this previous work in that it uses a multi-sensor array that gives an image with a high spatial resolution which, using a new mathematical analysis, can me more easily related to the structure of the cord damages.

2. DESCRIPTION OF THE SYSTEM

MYRIAD uses digital magnetic imaging to obtain a high-resolution image of the magnetic anomalies that occur above the steel cords in conveyor belts due to damages. The strength of the magnetic field depends on the structure of the cord damage and the belt-sensor distance. Typically, for distances of ~5cm, the magnetic field strengths above single cord breaks are only 1 to 5 times stronger than that of Earth's ambient field i.e. about 1 to 3 Gauss.

2.1 FRINGING MAGNETIC FIELD

Figure 1 shows a plot of the magnetic field lines above a broken magnetised cord. Due to the break, the left hand cord ends in a north pole and the right hand cord begins as a south pole. The plot at the bottom shows the vertical component of magnetic field, B_z, measured along the dashed line, L. The characteristic shape of this trace is typical of the signal that is detected by a magnetic field sensor when it is placed 2-4cm above a running belt. Considering the trace from left to right, initially at A, B_z~0, i.e. there is no field above intact cords. At B, the vertical component of the field has increased and reaches a maximum. B_z then decreases to zero in the centre of the break (between B and C) before decreasing to a minimum at C. Far away from the break, B_z again returns to zero. Interestingly, the polarity of the flux leakage signature is reversed at a splice (i.e. a negative going pulse is followed by a positive going one) due to the interleaving of the cords in the splice and hence a reversal of the adjacent N-S configuration. This characteristic difference in the signature suggests a novel way of differentiating between a splice and a cord break.

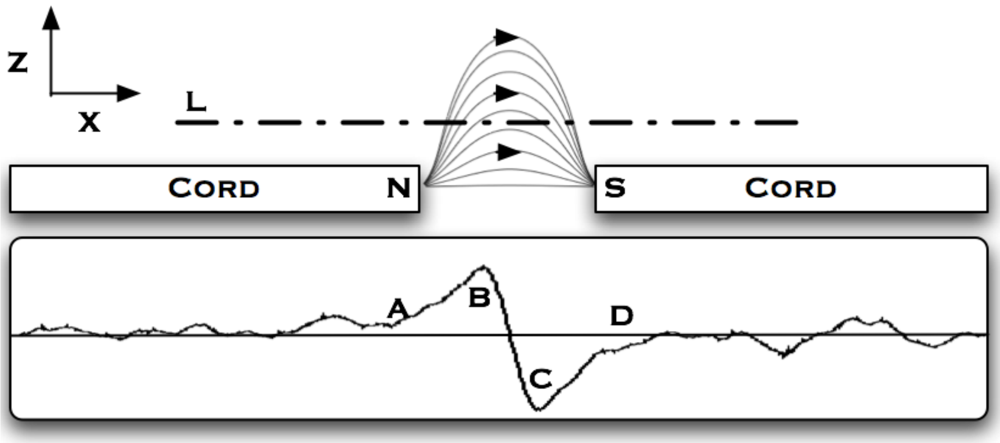

Figure 1. The top sketch shows the magnetic flux lines above the North and South poles of a cord break. The bottom plot shows the vertical z-component of the magnetic field, B_z, measured along the dashed line, L.

In order to obtain detailed measurements of the fringing field above the belt, a number of sensors are placed across its width. The first generation of magnetic systems developed up until now used relatively few (1 to 4) magnetic sensors. Example traces from such an array of 4 sensors are shown in Figure 2. Although it is clear that damage can be seen in trace 3, the transverse extent of the damage cannot be determined due to the sparse spacing of sensors across the belt width. In addition, the bipolar behaviour of the B-field trace is confusing and not easy to interpret by the unskilled operator who typically does not have a knowledge of electromagnetic theory. This technology solves both these problems by:

1. Using a large number (> 64) magnetic sensors arranged across the belt width. By having a number of sensors equal to ~2x the number of cords in the belt, individual cord breaks can be detected. In addition, if signals from adjacent independent channels behave in a similar way, there is more confidence that the magnetic field anomoly being detected by both sensors is real and not due to s noise spike.

2. Measuring one or more of the 3 components of the local fringing magnetic field above the belt can in principle be used to discover the configuration of the damaged cords using inverse modelling. In practice, the component perpendicular to the belt is found to be sufficient to describe the severity and extent of the damages.

3. Processing the raw magnetic field data using a mathematical transform to give a high-resolution image of the belt damages, which may be easily interpreted to determine their spatial extent and severity. The wavelet spatial spectrum of the magnetic anomalies gives a pseudo-color codes indication of the extent of the cord break. The transverse extent of this feature gives information about the number of cord breaks.

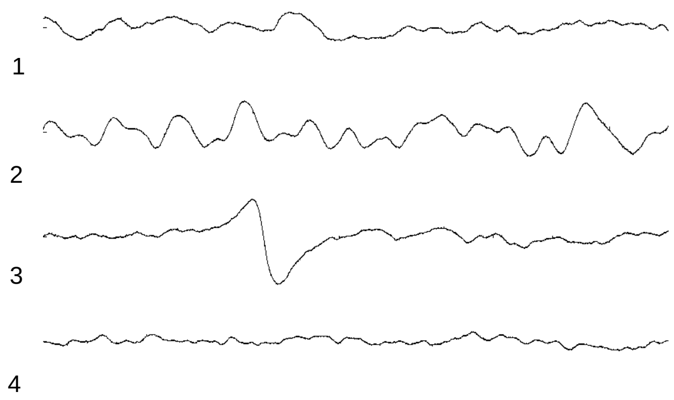

Figure 2. Plot of the magnetic field obtained from four equally spaced sensors (labelled 1 to 4) placed across the belt. This is the typical configuration for first generation magnetic systems.

2.2 CONFIGURATION

The experimental configuration comprises a set of permanent magnets that are placed across the width of the belt, and about 5 m upstream of the sensor array as shown in

Figure 3. After 2 to 5 revolutions of the conveyor, the cords have become sufficiently magnetised for splices and cord damages to be detected by the magnetic sensor array.

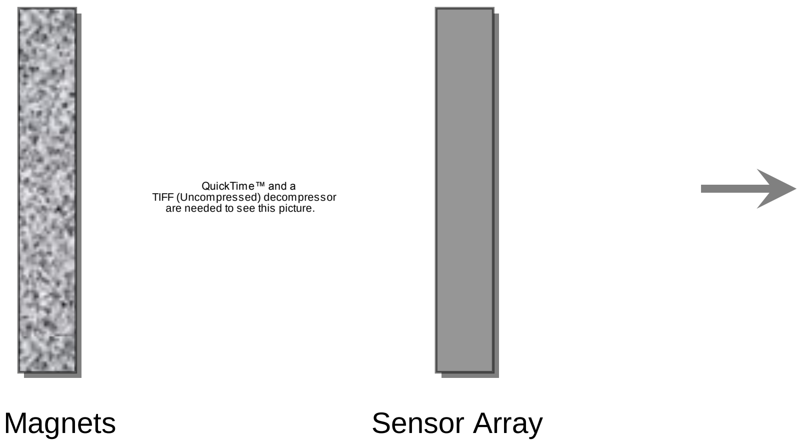

Figure 3. Plan view schematic of the experimental configuration. The arrow shows the direction of belt travel beneath the magnets and sensor array.

3. RESULTS

3.1 LABORATORY RESULTS

For the laboratory tests, a 7.2 m long, 750 mm wide, ST500 conveyor belt was set up in the laboratory (Figure 4). The belt is driven by a 1.75 kW variable speed drive giving belt speeds up to 5.2 m/s. For the laboratory tests, the belt speed was set to 3.5 m/s. This rig has been used to optimise the configuration of the permanent magnetic field, measure the response of different sensor transducers and different sensor arrays. Although this was an old belt that included some inherent damages, some additional artificial damages were created by cutting one or more cords, using an angle grinder.

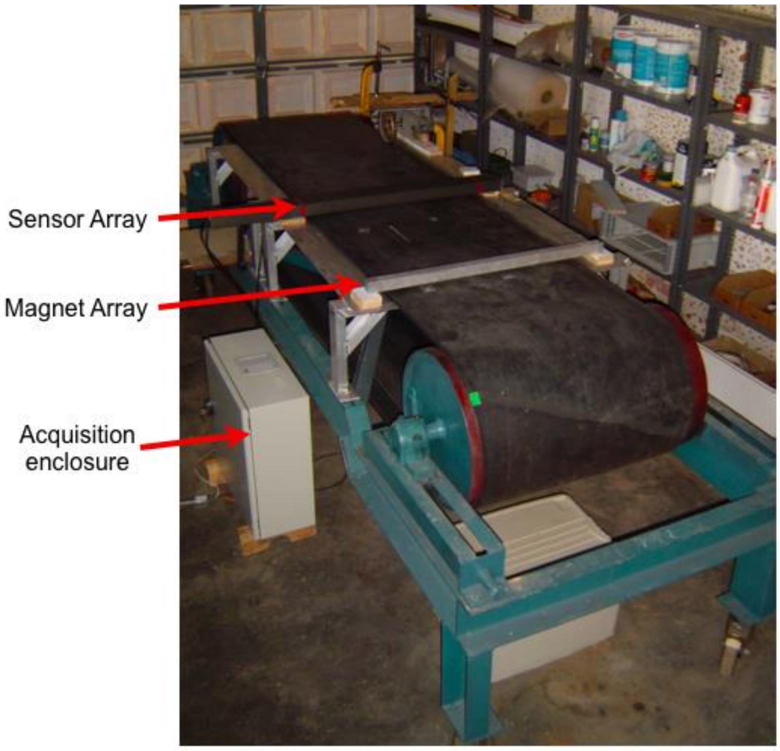

Figure 4. The test conveyor in the AIT laboratory. The belt is a 7.2 m long, 750 mm wide, ST500 belt mounted on 500 mm-diameter pulleys.

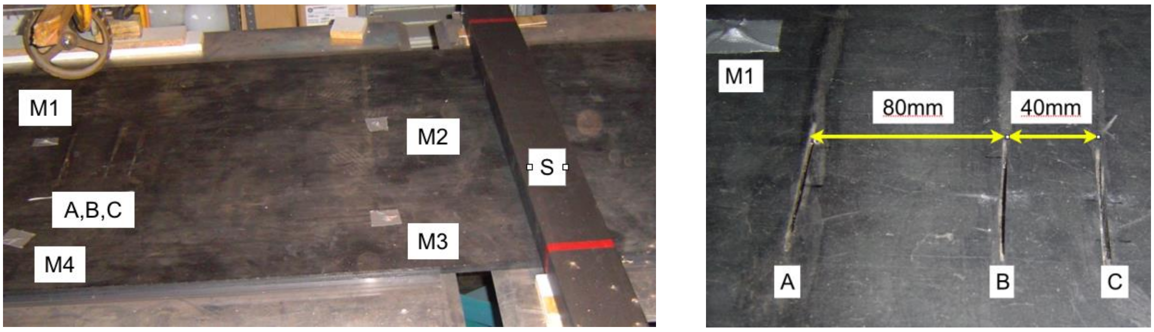

(a) (b)

Figure 5. (a) Test belt showing the magnetic markers (M1, M2, M3 & M4). S is the sensor array. (b) An enlargement of the damaged region showing marker M1 and artificial damages A, B and C.

The arrangement of the cuts A, B & C together with the four magnetic markers M1, M2, M3 & M4, are shown in Figure 5. The markers consist of small (3 mm) fragments of ceramic magnet that can be seen in both the X-ray and magnetic data, and were used to register the images in these two modalities. The artificial damages A, B & C resulted in 1½ -, 1- and 1½ -cut cords, respectively. In addition to these cord cuts, a ~8cm long cut was made in the rubber across the belt by the grinding disk. Both the rubber and cord cuts could be seen in the X-ray images but only the cord cuts could be seen in the magnetic images.

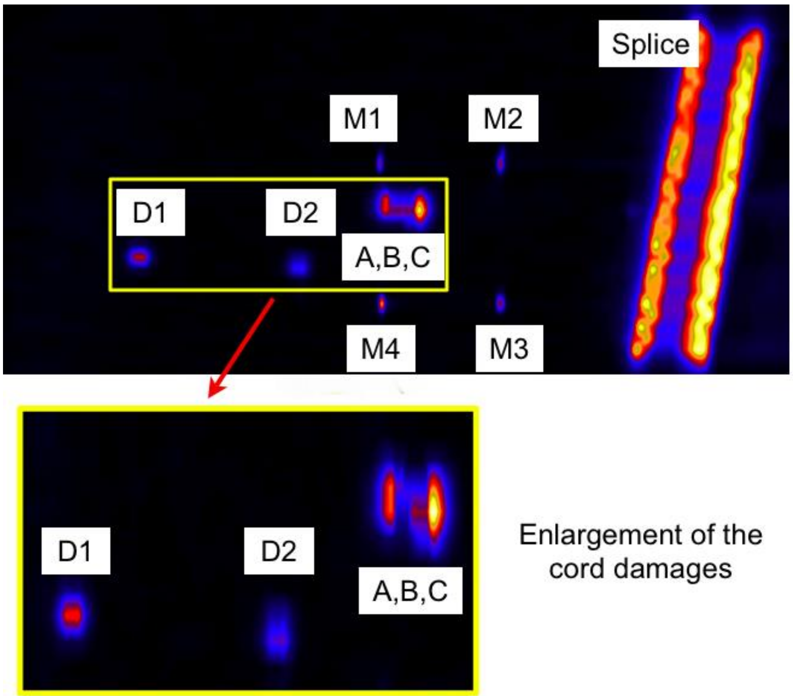

Figure 6. A magnetic image of the test belt showing the damages (D1 & D2 and A, B & C), markers (M1, M2, M3 & M4) and the splice. The damaged area is also shown enlarged.

Figure 6 shows a magnetic image of the damaged region of the belt after it had been processed by a wavelet transform. The markers, damages (A, B & C) as well as the splice can be clearly seen. Damage B is just visible between A and C in the enlarged inset. The sizes of the damage peaks in the transverse and longitudinal direction are proportional to the spatial extent of the damages themselves.

For this particular filter, the splice appears as two separate vertical columns of peaks. These peaks are more clearly displayed in the topographical representation of this data, shown in Figure 7, which is an alternative representation of the magnetic image data, shown in Figure 6.

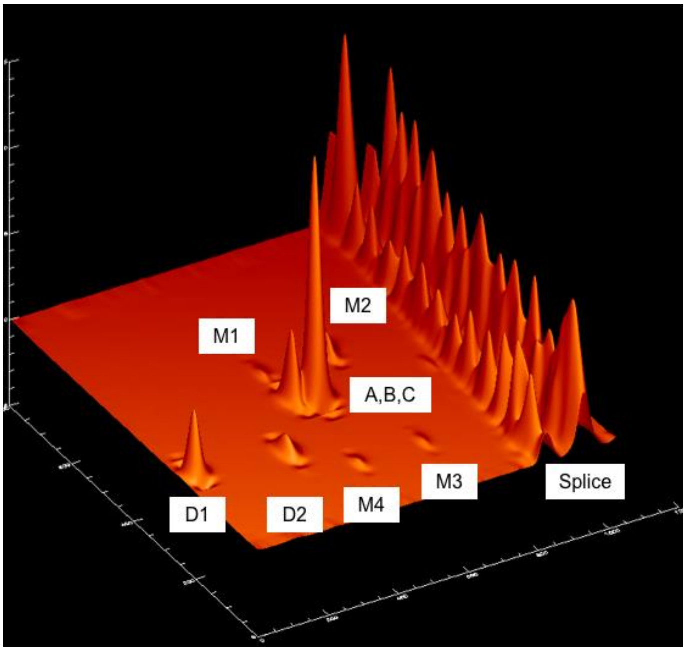

Figure 7. Topographic representation of the cord damage data showing the damages, magnetic markers and splice.

The additional damages, D1 and D2, corresponded to ~1cm visible cuts in the belt, and were not detected before the magnetic was taken, but were subsequently confirmed to be present in the X-ray images, described below in Section 3.2.

A careful study of the splice in Figure 7 indicates that it appears as two adjacent columns of peaks, with each peak corresponding to an end of a cord in the splice. The peaks in each column are staggered with respect to the corresponding peaks in the adjacent column due to the interleaved nature of the individual cords in the splice. This high degree of spatial detail suggests that individual splices (and possibly splice stretch) can also be monitored.

3.2 X-ray Validation

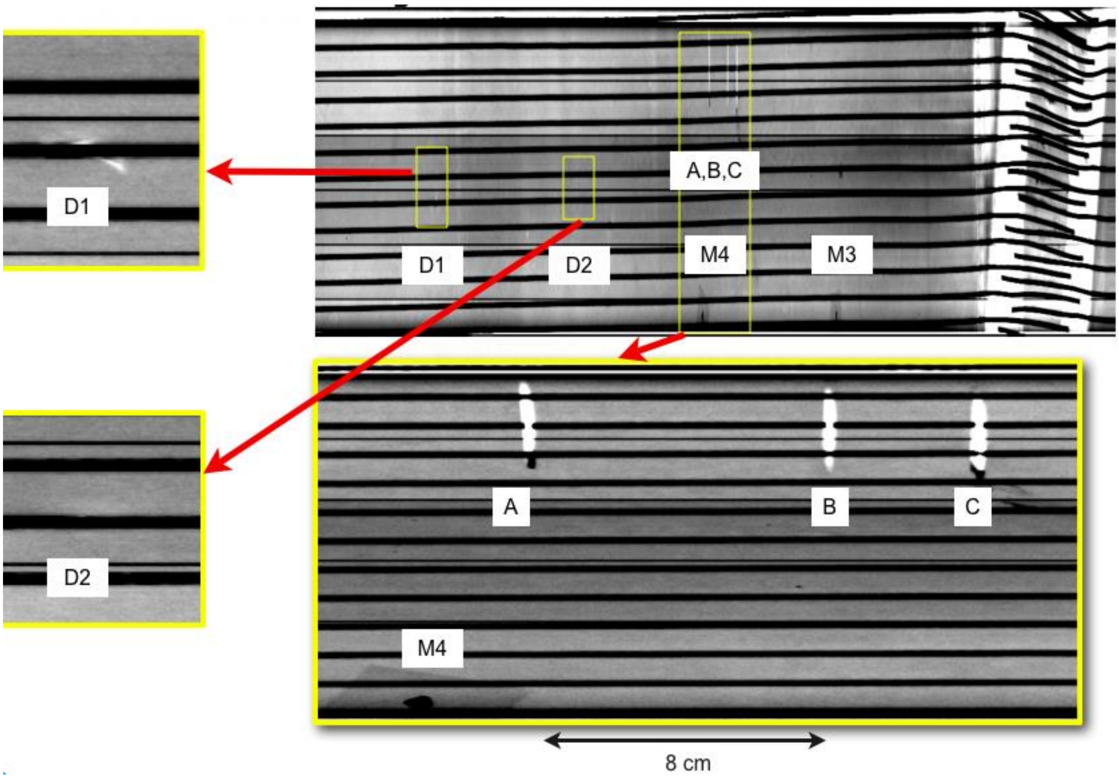

Figure 8. X-ray images of the damages on the test belt. The areas corresponding to missing rubber appear as bright vertical stripes in damages A, B & C.

The magnetic images have been validated against X-ray imaging as shown in Figure 8. The cuts A, B and C are clearly visible since they show up as bright vertical line segments (due to the missing rubber) at the centre of which are the cord breaks. The inherent damages, D1 & D2, appear to correspond to both rubber and cord damage. D2 is only just visible in the X-ray image and appears to be due to either single strand or cord corrosion.

3.3 FUTURE WORK

Although MYRIAD has been fully tested in the laboratory, a comprehensive beta test site schedule is necessary in order to evaluate the technology when it is subjected to an industrial environment, and to validate the magnetic damage images against X-ray images. This will confirm that both the damage severity and location can be equivalent to the information obtained from X-ray imaging.

A full software suite is also needed to provide a user interface and keep an archive of historical images, so that trending can be analysed. The software should also have a real-time functionality so that it can provide both critical and non-critical alarm signals to PLCs.

At the time of writing, a prototype has been installed at a beta test site and has been running for the past 3 months. A number of data sets have been collected and are being used to develop a realtime monitoring capability. Besides announcing an alarm when a damage above a certain threshold has been detected, it is hoped that the growth of the damage severity can also be monitored.

4. SUMMARY AND CONCLUSIONS

By measuring the fringing magnetic fields above a magnetised steel cord conveyor belt with a multi-sensor array, it has been possible to produce a high-resolution image of cord damages and belt splices. A wavelet analysis of this data makes it possible to quantify both the position and spatial extent of the damages, which is required for continuous belt condition monitoring. Furthermore, it has been demonstrated that, since it is possible to see the individual ends of the cords in a splice, it is also possible to monitor individual splices. MYRIAD is currently being evaluated at a beta test site in South Africa.

5. REFERENCES

1. MJ Alport, JH Fourie, JF Basson, T Padayachee; "Condition Monitoring of Fabric-Reinforced Conveyor Belting using Digital X-ray Imaging"; Beltcon 13 International Materials Handling Conference, Mintek Conference Centre, 3-4 August 2005, Strijdom Park, Johannesburg, South Africa.
2. A. Harrison; "Magnetic detection of air gaps formed at breaks in conveyor belt cards"; US Pat. 4864233 (Filed 1 August 1985).
3. "Condition Monitoring of Steelcord-Reinforced Conveyor Belts"; South African Provisional Patent Number 2007/00760 (Filed 25 January 2007).

6. ACKNOWLEDGEMENTS

Advanced Imaging Technologies (Pty) Ltd acknowledges financial support received from The Innovation Fund, Department of Science and Technology.

7. AUTHORS' CVS. PAPER TO BE PRESENTED BY MJ ALPORT.

7.1 CURRICULUM VITAE OF MJ ALPORT

Qualifications:

- BSc (Hones) (Physics) 1974, University of Natal, Durban.
- MSc (Physics) 1975-1977, University of Natal, Durban.
- PhD (Plasma Physics) 1977-1981, University of Iowa (USA).

Experience:

- 1978 → 2000: Visiting scientist at Laboratoire de Mécanique des Fluides, Grenoble, France; University of Groningen, Nuclear Physics Department, KVI; Dept. of Physics, West Virginia University, Morgantown; Dept. of Nuclear Engineering and Engineering Physics, University of Wisconsin, Madison, Wisconsin; Laboratory for Plasma and Fusion Energy Studies, University of Maryland, College Park, MD; Dept. of Physics and Astronomy, University of Iowa, Iowa City, Iowa.
- 1981 → present: Associate Professor and Head of the Applied Physics Group. School of Physics, University of KwaZulu-Natal, Durban.
- 2004: Founder and MD of Advanced Imaging Technologies (Pty) Ltd.

7.2 CURRICULUM VITAE OF JF BASSON

Qualifications:

- BSc (Physics, Mathematics) 1998, University of Natal, Durban.
- BSc (Hones) (Physics) 1999, University of Natal, Durban.
- MSc (Physics) 2001, University of Natal, Durban.
- PhD (Astrophysics) 2003, University of Cambridge (UK).

Experience:

- March 2003 → December 2003: Consulting Physicist for the Applied Physics Group at the University of Natal.

- January 2004 → Present: Consulting Physicist for Advanced Imaging Technologies (Pty) Ltd.

7.3 CURRICULUM VITAE OF T PADAYACHEE

Qualifications:

- MSc (Applied Physics) 2001, University of Natal, Durban.
- BSc (Hones) 1997, University of Natal, Durban.
- BSc (Applied Mathematics, Physics) 1996, University of Natal, Durban.

Experience:

- 1995 → 1997: Vacation work at DebTech in Johannesburg, mainly in the field of X-ray and Gamma Spectroscopy.
- January 1998 → December 1999: Assistant Research Officer at DebTech. Project experience included X- and Gamma-ray Spectroscopy, X-ray Computed Tomography, X-ray Digital Radiography, Neutron Activation Analysis, X-ray Fluorescence and Infrared Reflectance Spectroscopy.
- January 2004 → Present: Consulting Physicist for Advanced Imaging Technologies (Pty) Ltd.

7.4 ADDRESS OF AUTHORS

MJ Alport, JF Basson, T Padayachee
Suite #307, Private Bag X04, Dalbridge, 4014, South Africa
Tel: +27 (0)31 202-5528
Fax: +27 (0)31 202-5527
e-Mail: Alport@ait-sa.com
Web: www.AIT-SA.com